

CFD Analysis of the Slippage Effects on Elastohydrodynamic Lubrication in Line Contact Problem

S. Srirattayawong*, R. Aungkurabut

School of Engineering, University of Phayao

*Corresponding author E-mail : Sutthinan.sr@up.ac.th

(Received: October 19, 2017, Revised: September 14, 2018, Accepted: October 24, 2018)

Abstract

In this paper, the effects of a slippage on an elastohydrodynamic lubrication (EHL) in line contact problem using an advanced computational fluid dynamics (CFD) model are presented. A cylindrical roller is assumed to be infinitely long and rotates on a plate under an applied load. In addition, the no-slip and slip boundary conditions were defined between lubricant and solid walls. The Navier-Stokes and the elasticity equations were solved simultaneously. The Ree-Eyring model was used to calculate the viscosity of lubricant. The developed CFD model had been applied to the series of cases of lubricated slippage effect with the applied loads $L=1.5$ kN and 2.5 kN, slide-to-roll ratios: $SRR=0, 1$ and 2 under the thermal condition. The flow characteristics in the CFD model such as the pressure distribution, the fluid film thickness, the velocity of fluid flow, the viscosity and the temperature distribution were investigated. To illustrate, the developed CFD model is successively to simulate the EHL line contact problem, and can deal with the slippage problem. The simulation results show that the slippage effect is significant to the EHL problem, especially in the case of pure sliding.

Keywords: EHL, slippage, lubrication, CFD, Non-Newtonian.

1. NOMENCLATURE

E	[Pa]	Reduced modulus of elasticity
f	[‐]	Volume fraction
h_o	[m]	The minimum film thickness
h_i	[m]	Film thickness
L	[Nm ^{‐1}]	Applied load per unit width
p	[Pa]	Pressure
p_{sat}	[Pa]	Liquid saturation vapor pressure
R	[m]	Reduced radii of curvature
$R(i)$	[m]	Surface roughness term
SRR	[‐]	Slide to roll ratio = $2[u_p - R_c w_c]/(u_p + R_c w_c)$
T	[K]	Temperature
Δt	[s]	Time step
u	[m/s]	Velocity
V_{ch}	[‐]	A characteristic velocity
x_i	[m]	Cartesian axis in i direction
z	[‐]	Viscosity index
Special character		
α_i		Volume fraction of phase
ρ	[kg/m ³]	Density
τ	[Pa]	Viscous stress tensor
β	[1/K]	Thermal expansivity of lubricant
η	[Pa·s]	Viscosity of Newtonian fluid
η_b	[Pa·s]	Viscosity at ambient pressure
ψ	[m]	Slippage length
Subscripts		
c		Cylinder
p		Plate
in		At the inlet position
out		At the outlet position
o		Ambient or reference
l		Liquid phase
v		Vapor phase
m		Mixture phase
sat		Saturation vapor pressure

2. INTRODUCTION

The lubrication system plays an important role in machines as it can help reduce friction force, as well as prevent and reduce the wear that can occur to all contacting and moving parts. Thus, lubricants have received much interest over the years as it is the lifeblood of all mechanical machines, especially in sliding and rolling elements under heavy loads.

Many researchers have developed different methods, simple or complex for solving lubrication problems. All studies in fluid film lubrication were start up from the 1880s, when a combination of experiments was followed by a unifying mathematical theory. Osborne Reynolds [1] presented the differential equation that is used to state the relationship between the motion and viscosity of the lubricant. The Reynolds equation has been used to describe laminar flows for Newtonian fluids in hydrodynamics lubrication problems for example a thin film in gear [2, 3]. Later, some models were suggested for improving the Reynold equation such as elastic deformations due to the contact pressures [4], a pressure–viscosity effect [5]. After that time, the development and understanding of elastohydrodynamic lubrication (EHL) have been presented. Petrushevich [6] solved the elastohydrodynamic lubrication problem (EHL) for the line contact problem and got the full numerical solution. The result indicated that the pressure profile increased gradually at the lubricant inlet region of contact and reaches maximum pressure forming a pressure spike at the minimum film thickness. This character is known as the ‘Petrusevich Pressure Spike’. Later, outstanding contributions have been accomplished by numerous investigators. Many numerical techniques were proposed to the EHL problems [7-12]. An analytical method derived from the combination of lubricant properties

(density and viscosity) and the classic Reynolds equation were presented [13]. It is well known as the ‘generalized Reynolds equation’. Earlier, the isothermal theories have been achieved [14]. Then, the Reynolds equation was improved to be more realistic by considering thermal effect [15-18], non-Newtonian fluid [18-22], transient effect [23, 24] and surface roughness [25-29]. Recently, a CFD technique has been used to simulate an EHL line contact problem instead of the Reynolds equation [30-35].

It can be seen from the above literature reviews that the study of the thin film lubrication problem has been continually developed. The intent of this paper is an endeavour to establish a framework for understanding the slippage effects on to the EHL in line contact problem using the CFD technique.

3. METHOD

In order to explore and analysis the characteristic of EHL problem, it is necessary to design a CFD model such as geometry, boundary conditions and physical properties. In this paper, the 2D CFD model is created for the proposed EHL in line contact problem. The cylindrical roller is assumed to be infinitely long and rotates on the plate, thus the pressure distribution of the z direction can be considered to be uniform. Therefore, only the pressure distribution of the front plane is investigated and presented. The boundary conditions and geometry model are maintained the same in all study cases. To identify the slippage effects, the slip boundary condition is applied at the plate to compare with a no-slip boundary condition.

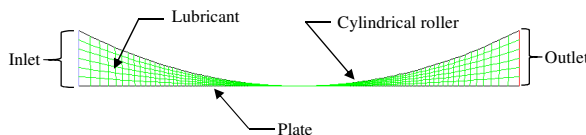


Figure 1 Schematic of the CFD model

In this research, the ICEMCFD software is used to create the CFD model of the EHL problem, as shown in Figure 1. Then meshes are generated in the geometry. The proposed CFD model is examined by completing the mesh dependent test to ensure that the resolution is adequate. The spacing of the mesh in the CFD model is refined from $0.5 \mu\text{m}$ to $0.25 \mu\text{m}$ and $0.167 \mu\text{m}$. It is found that the predicted pressure distributions with the mesh spacing of $0.50 \mu\text{m}$, $0.25 \mu\text{m}$ and $0.167 \mu\text{m}$ are the same. Then, the maximum mesh size of $0.25 \mu\text{m}$ was chosen and applied to the contact zone of the CFD model in this study.

Table 1: The common data using in the CFD model

Parameters	Value	Unit
Input data		
- An applied load, W	1.0, 1.5, 2.5	kN/m
- Average velocity, U_a	2.5	m/s
- Slide to roll ratio (SRR)	0, 1, 2	-
Solid properties (Cylindrical roller and plate)		
- Elastic modulus of solids, E_1, E_2	2.1×10^{11}	Pa
- Poisson's ratio of solids, ν_1, ν_2	0.30	-
- Specific heat of solids, C_{p1}, C_{p2}	460	J/Kg-K
- Density of solids, ρ_1, ρ_2	7,850	kg/m ³
- Thermal conductivity, k_1, k_2	47	W/m-K
- Radii of curvature (Cylindrical roller)	0.01	m
Lubricant properties		
- Inlet viscosity of lubricant, η_0	0.01	Pa-s
- Vapour dynamic viscosity, μ_v	8.97×10^{-6}	Pa-s
- Liquid density, ρ_l	846.0	kg/m ³
- Vapour density, ρ_v	0.028	kg/m ³
- Thermal conductivity of lubricant, k	0.14	W/m-K
- Temperature-viscosity coefficient of lubricant, γ	0.0476	1/K
- Specific heat of lubricant, C_p	2,000	J/ Kg-K
- Thermal expansivity of lubricant, β	6.5×10^{-4}	1/K
- Pressure-viscosity coefficient, z	0.689	-

The minimum gap between the cylindrical roller and the plate is 0.1 mm. The quad-mesh type is employed to generate meshes for the CFD model. There are 20,517 nodes in total. Then the CFD model is solved using the commercial software ANSYS Fluent 12.

4. THEORY

In the analysis of thin fluid film lubrication, the CFD approach is used to calculate the velocity and pressure in fluid flow at the narrow gap between the top cylindrical roller and the plate instead of the Reynolds equation. The fluid solver and solid solver are employed. It is a coupling between the fluid flow (lubricant) and the deformation of the solid part.

The characteristics of fluid flow can be explained by the conservation form of the fluid flow. This combines the continuity equation and momentum equation which can be written in the general form:

Conservation of mass:

$$\frac{\partial \rho}{\partial t} + \nabla \cdot (\rho \mathbf{u}) = 0 \quad (1)$$

Conservation of momentum:

$$\frac{\partial(\rho \mathbf{u})}{\partial t} + \nabla \cdot (\rho \mathbf{u} \mathbf{u}) = -\nabla p + \nabla \cdot \tau \quad (2)$$

$$\text{where } \tau = -\eta (\nabla \mathbf{u} + (\nabla \mathbf{u})^T) + \frac{2}{3} \eta \mathbf{I} \nabla \cdot \mathbf{u} \quad (3)$$

Conservation of energy:

$$\frac{\partial(\rho T)}{\partial t} + \nabla \cdot (\rho \mathbf{u} T) = \nabla \cdot (k \nabla T) + S_r \quad (4)$$

$$\text{where } S_r = Q_{\text{shear}} + Q_{\text{compress}} \quad (5)$$

$$Q_{\text{shear}} = \eta \left(\nabla \mathbf{u} : \nabla \mathbf{u} + \nabla \mathbf{u} : (\nabla \mathbf{u})^T - \frac{2}{3} (\nabla \cdot \mathbf{u})^2 \right) \quad (6)$$

$$Q_{\text{compress}} = -\frac{T}{\rho} \left(\frac{\partial \rho}{\partial T} \right) (\mathbf{u} \cdot \nabla p) \quad (7)$$

The density of lubricant (ρ) is a pressure dependent. It is well known that the generated pressure in the contact zone is very high. For that reason, this effect cannot be neglected. As Dawson and Higginson presented, there was a linear variation on pressure and density [11]. The relation between pressure and density can be stated as follows:

$$\rho_i = \rho_0 \left(1 + \frac{0.59 \times 10^{-9} p_i}{1 + 1.7 \times 10^{-9} p_i} \right) \left[1 - \beta(T - T_0) \right] \quad (8)$$

where β is thermal expansivity of lubricant.

The viscosity of lubricant also depends on the pressure as well as the density. The increasing of the viscosity with pressure can be calculated as proposed by Roelands and Houpert [12].

$$\eta_{Houpert} = \eta_0 \exp \left\{ \left[\ln \eta_0 + 9.61 \right] \left[-1 + \left(1 + 5.1 \times 10^{-9} p_i \right)^2 \right] \left[\frac{T-138}{T_0-138} \right] - c(T-T_0) \right\} \quad (9)$$

$$\text{where } c = (\ln \eta_0 + 9.61) \left(1 + 5.1 \times 10^{-9} p_i \right)^2 \left(\frac{S_0}{T_0-138} \right) \quad (10)$$

$$S_0 = \gamma \left(\frac{T_0-138}{\ln \eta_0 + 9.61} \right) \quad (11)$$

and

$$\eta_{Eyring} = \frac{\tau_0}{\dot{\gamma}_{eq}} \sinh^{-1} \left(\frac{\eta_0 \dot{\gamma}_{eq}}{\tau_0} \right) \quad (12)$$

The Ree-Eyring model can be used to present the viscosity in each cell. It depends on the equivalent shear rate as the following conditions;

$$\eta_i = \begin{cases} \eta_{Houpert}, & \dot{\gamma}_{eq} < 10^{-5} \\ \eta_{Eyring}, & \dot{\gamma}_{eq} \geq 10^{-5} \end{cases} \quad (13)$$

The cavitation effect [39] is not modelled by the Reynolds equation. However, the occurred negative pressure in conjunction zone can be solved by applying a cavitation model to the CFD model for the EHL problem. The full cavitation model [13] has been employed in this research is:

$$\frac{\partial(\rho_m f)}{\partial t} + \nabla(\rho_m \vec{v}_f) = \nabla(\gamma \nabla f) + A - B \quad (14)$$

where A and B are given by

$$A = 0.02 \frac{V_{ch}}{\sigma} \rho_i \rho_v \sqrt{\frac{2(p_{sat} - p)}{3\rho_i}} (1 - f) \quad (16)$$

$$B = 0.01 \frac{V_{ch}}{\sigma} \rho_i \rho_v \sqrt{\frac{2(p - p_{sat})}{3\rho_i}} (f) \quad (17)$$

The density of a lubricant for a liquid phase is a function of pressure as defined in equation (8). Thus the density of the vapor phase should be calculated from the fraction equation. Therefore the density of a mixture phase can be written as:

$$\rho = \alpha_v \rho_v + \alpha_g \rho_g + (1 - \alpha_v - \alpha_g) \rho_l \quad (18)$$

The local lubricant film thickness or the gap at the contact zoned can be calculated by a geometric equation. The geometry of the contacting elastic solids is defined as shown in Figure 1. The full-film lubrication is assumed in this study. Then the lubricant film thickness is depended on the physical geometry of the cylindrical roller and the elastic deformation term [36] which is governed by the pressure distribution of the contact [37].

$$h_i = h_o + \frac{x^2}{2R} + R(i) - \frac{2}{\pi E} \int_{-\infty}^{x_i} p(\xi) \ln(x - \xi)^2 d\xi \quad (19)$$

The gap between the cylindrical roller and the bottom plate must be corrected in each iteration and updated until the generated pressure is equal to the applied load. Then, the constant h_o can be solved using a force balance equation [38].

$$h_o^{new} = h_o^{old} + defect \quad (20)$$

$$\text{where } defect = L - \int_{-\infty}^{\infty} p_i dx$$

As the cylindrical roller and plate surfaces are defined to be moving with different velocity. Especially, in case of high SRR , the shear strain is very high. Then the lubricant can be slipped along a solid-liquid interface. This phenomenon can be calculated by:

$$u_f = \psi \frac{\partial u_s}{\partial z} \Big|_{wall} \quad (21)$$

where u_s indicates the streamwise slippage velocity at the hydrophobic surface.

5. NUMERICAL METHOD

The finite-volume method is used in this study. The integral form of the transport equations (1) and (2) has to be applied to a discretized equation. The geometry domain is subdivided into a finite number of subdomain as shown in Figure 1.

The pressure and velocity variables in the domain are calculated by using the PISO algorithm. In addition, the spatial discretization methods are applied to the CFD model such as least square cell base, second order, second order upwind, and quick for calculating the gradient, pressure, density and momentum, respectively. Then the transport equation in a general form can be used to solve iteratively for all cells in the domain, as demonstrated below:

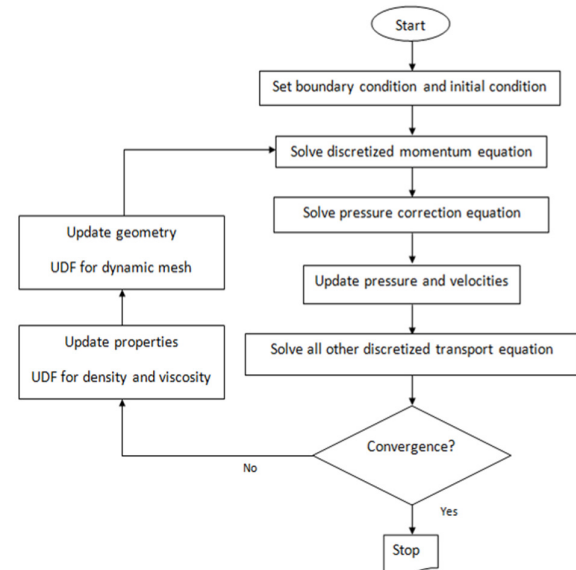


Figure 2 The flow chart for solving the EHL problem of the CFD model

At the beginning of the iteration process, the velocity and pressure fields are approximated. Then these parameters are used to solve the momentum equation and the pressure correction equation. These values will be corrected in each iteration, until the acceptable convergence of pressure and velocity is achieved as shown in Figure 2.

6. RESULTS AND DISCUSSION

The results of the proposed CFD model were compared with that from the Reynolds equation presented by Chu et al [40]. Figure 3 depicts that the pressure distribution and the film thickness of both methods are in good agreement [41]. It can be clearly seen that the characteristics of EHL problem can be simulated by using the CFD technique very well.

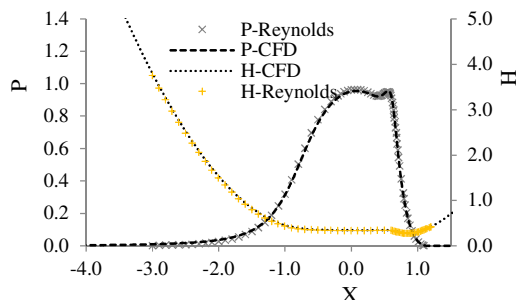


Figure 3 Comparison of dimensionless film thickness (H) versus pressure distribution (P) between the CFD model and the Reynolds equation

The simulation results of two parameters varied are presented in this paper. The first case shows the effect of slippage with the ratio of the different velocity between the cylinder and the plate (*SRR*) varied. Then the second case presents the slippage influences with the applied load varied.

Figures 4, 5 and 6 show the effects of slippage on the pressure distribution and the fluid film thickness at the contact zone when *SRR*=0, 1 and 2, respectively. It is found that the slippage condition is significantly to the characteristics of the EHL problem. The effect of slippage is increased when the *SRR* between the plate and the cylinder was increased. The pressure distribution of the slippage case of *SRR*=1 and 2 is clearly higher than the no slippage case. This is due to the fact that the film thickness of the slippage case is thinner than the no slippage case as shown in Figure 6.

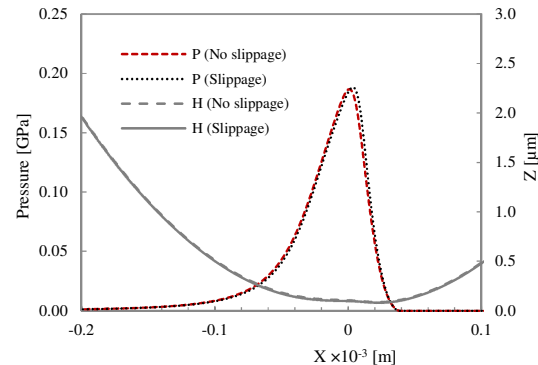


Figure 4 Comparison of pressure distributions and film thicknesses between no slippage and slippage when *SRR*=0 and *L*=1 kN/m

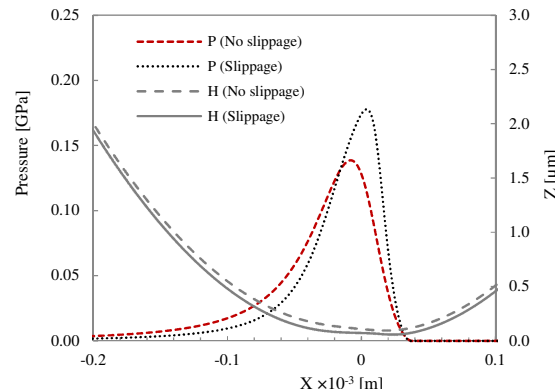


Figure 5 Comparison of pressure distributions and film thicknesses between no slippage and slippage when *SRR*=1 and *L*=1 kN/m

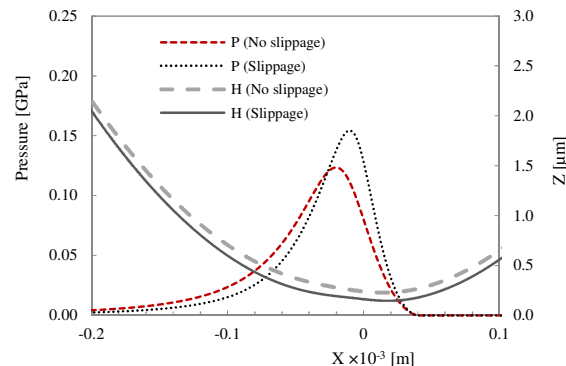


Figure 6 Comparison of pressure distributions and film thicknesses between no slippage and slippage when *SRR*=2 and *L*=1 kN/m

Some results illustrate that the effect of slippage on the EHL problem is very small when the applied load was increased for the *SRR* = 0 (no slide between both solid surfaces). Figure 7 shows the comparison of the pressure distributions and the fluid film thickness profiles between no slippage and slippage applied for the plate when *L*=1.5 kN/m and 2.5 kN/m. It is found that the pressure distribution and the fluid film thickness are quite similarly in either case. However, the comparison of

pressure distribution is different when the *SRR* increased as presented in Figure 7. It can be clearly seen that the slide to roll ratio is significant on the slipped wall condition.

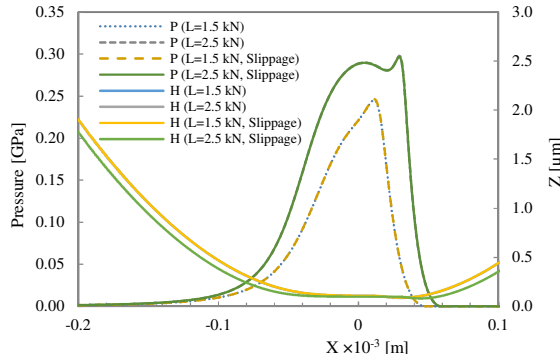


Figure 7 Comparison of pressure distributions and film thickness profiles between no-slipage and slippage when $L=1.5 \text{ kN/m}$, 2.5 kN/m and $SRR=0$

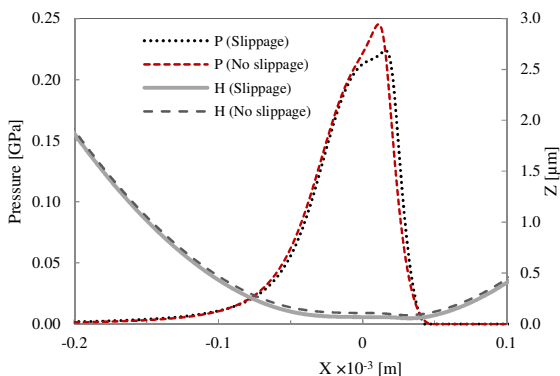


Figure 8 Comparison of pressure distributions and film thickness profiles between no-slipage and slippage when $L=1.5 \text{ kN/m}$, and $SRR=1$

Figures 9-13 reveals the behaviour of thin fluid film lubrication when the slippage effect considered. The cylindrical roller was rotated around 125 rad/s . while the plate was moved with $v=3.75 \text{ m/s}$. It explores that the cylinder is more influent on lubricant velocity than the plate as shown in Figure 9. This is because the lubricant was slipped from the solid wall (Plate). Therefore, in this case, the velocity of lubricant is dominated by the velocity of the cylindrical roller.

Figure 10 shows the contour of the pressure distribution of the lubricant at the conjunction zone. The maximum pressure is about 1.6 MPa . The pressure very high because the fluid film is very thin. The shear stress and shear rate of the layer of fluid film near the cylinder are higher than the plate where the slip wall condition was applied as shown in Figures 11 and 12.

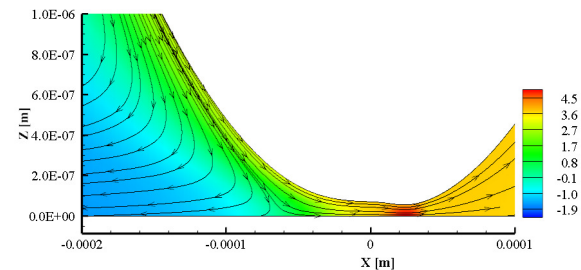


Figure 9 The contours of lubricant velocity [m/s]

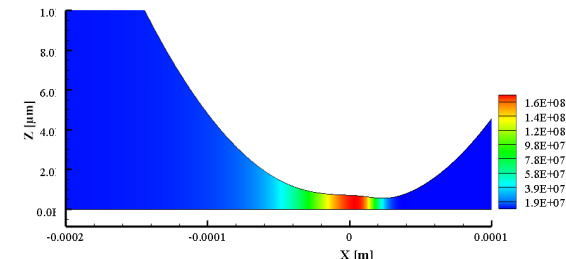


Figure 10 The contours of static pressure [Pa]

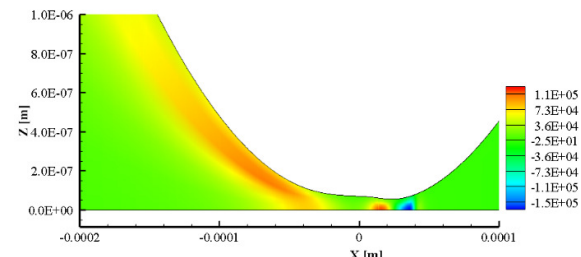


Figure 11 The contours of velocity gradient, du/dx [s^{-1}]

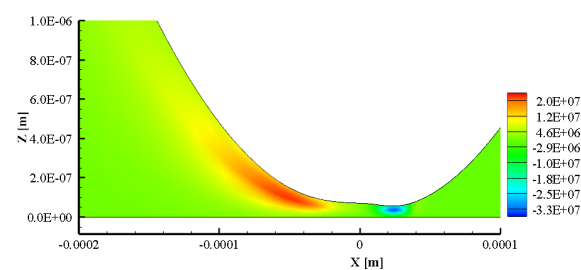


Figure 12 The contours of velocity gradient, du/dz [s^{-1}]

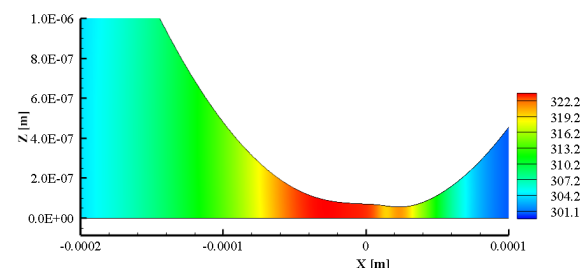


Figure 13 The contours of temperature [K]

Figure 13 presents the temperature contour at the contact zone. The temperature rises because the heat sources were generated by the Q_{shear} and Q_{compress} terms as presented in equations (6) and (7).

7. CONCLUSION

An advanced 2D CFD model has been successfully developed for simulating the characteristics of the EHL line contact problem, with a focus on the effects of slippage condition. The CFD model has been used successively to simulate the pressure distribution, the generated temperature, and the velocity of lubricant under the varied slide to roll conditions. The results show that the CFD model can be a useful tool for the EHL line contact problem, and can deal with the slippage problem. The main findings are summarized below:

- The slippage condition is a very important factor that affects the shear strain, especially for the case of pure sliding ($SRR=2$).
- The fluid film thickness is thinner than the no slippage case.

8. ACKNOWLEDGMENT

The author gratefully acknowledge the financial support on the project from the Ministry of Science and Technology of Thailand and the University of Phayao.

9. REFERENCES

[1] O. Reynolds, (1886), "On the theory of lubrication and its application to Mr. Beauchamp Tower's experiments, including an experimental determination of the viscosity of olive oil", *Philosophical Transactions of the Royal Society of London*, vol. 177, pp. 157-234.

[2] H. Martin, (1916), "Lubrication of gear teeth," *Engineering*, London, vol. 102.

[3] L. Gümbel, (1916), "Über Geschmierte Arbeitsräder (On the Lubrication of Gears)", *Zeitschrift für das Gesamte Turbinenwesen*, vol. 13.

[4] A. Meldahl, (1914), "Contribution to the Theory of the Lubrication of Gears and of the Stressing of the Lubricated Flanks of Gear Teeth", *Brown Boveri Review*, vol. 28, pp. 374-382.

[5] A. von Mohrenstein-Ertel, (1949), "Die Berechnung der Hydrodynamischen Schmierung Gekrümmter Oberflächen unter Hoher Belastung und Relativbewegung", *Fortschrittsberichte VDI*, vol. Ser. 1, No. 115.

[6] A. I. Petrusevich, (1951), "Fundamental conclusions from the contact-hydrodynamic theory of lubrication", *Izv. Akad. Nauk. SSSR (OTN)*, vol. 2, p. 14.

[7] D. Dowson and G. R. Higginson, (1959), "A numerical solution to the elasto-hydrodynamic problem", *Journal of Mechanical Engineering Science*, vol. 1, pp. 6-15.

[8] M. E. Muller, (1958), "An inverse method for the generation of random normal deviates on large-scale computers", *Mathematics of Computation*, vol. 12, pp. 167-174.

[9] H. S. Cheng and B. Sternlicht, (1965), "A Numerical Solution for the Pressure, Temperature, and Film Thickness Between Two Infinitely Long, Lubricated Rolling and Sliding Cylinders, Under Heavy Loads", *Journal of Basic Engineering*.

[10] C. H. Venner, (1991), "Multilevel Solution of the EHL Line and Point Contact Problems", PhD, University of Twente, Enschede, Netherlands.

[11] A. A. Lubrecht, (1987), "Numerical solution of the EHL line and point contact problem using multigrid techniques", Ph.D. Thesis, University of Twente, Enschede, Netherlands.

[12] H. Okamura, (1983), "A contribution to the numerical analysis of isothermal elastohydrodynamic lubrication", *Proc. 9th Leeds-Lyon Symp. on Tribology*, pp. 313-320.

[13] D. Dowson, (1962), "A generalized Reynolds equation for fluid-film lubrication", *International Journal of Mechanical Sciences*, vol. 4, pp. 159-170.

[14] D. Dowson, G. Higginson, and A. Whitaker, (1962), "Elasto-hydrodynamic lubrication: a survey of isothermal solutions", *Journal of Mechanical Engineering Science*, vol. 4, pp. 121-126.

[15] L. Houpert, (1985) "New results of traction force calculations in ehd contacts", *Trans. ASME, J. Lub. Tech.*, vol. 107, p. 8.

[16] C. J. A. Roelands, (1966), "Correlational Aspect of Viscosity-Temperature-Pressure Relationships of Lubricating Oils", PhD Thesis, Delft University of Technology, Netherlands.

[17] B. Sternlicht, P. Lewis, and P. Flynn, (1961), "Theory of lubrication and failure of rolling contacts", *Journal of Basic Engineering*, vol. 83, p. 213.

[18] P. C. Sui and F. Sadeghi, (1990), "Thermal Elastohydrodynamic Lubrication of Rolling/Sliding Contacts", *Trans. ASME, Jour. Trib.*, vol. 112, p. 6.

[19] K. L. Johnson and J. L. Tevaarwerk, (1977), "The shear behaviour of elastohydrodynamic oil films", *Proc. R. Soc. London*, vol. A. 356, pp. 215-236.

[20] Y. Peiran and W. Shizhu, (1990), "A generalized Reynolds equation for non-Newtonian thermal elastohydrodynamic lubrication", *Journal of tribology*, vol. 112, pp. 631-636.

[21] S. H. Wang, D. Y. Hua, and H. H. Zhang, (1988), "Full numerical EHL solution for line contacts under pure rolling condition with a non-Newtonian rheological model", *Journal of Tribology*, vol. 110, pp. 583-586.

[22] S. P. C. and F. Sadeghi, (1991), "Non-Newtonian Thermal Elastohydrodynamic Lubrication", *Trans. ASME, Jour. Trib.*, vol. 113, p. 6.

[23] S. Bair, J. a. Jarzynski, and W. O. Winer, (2001), "The temperature, pressure and time dependence of lubricant viscosity", *Tribology International*, vol. 34, pp. 461-486.

[24] K. F. Osborn and F. Sadeghi, (1992), "Time Dependent Line EHD Lubrication Using the Multigrid/Multilevel Technique," *ASME. Journal of Tribology*, vol. 114, pp. 68-74.

[25] X. Ai and H. S. Cheng, (1994), "A Transient EHL Analysis for Line Contacts With Measured Surface Roughness Using Multigrid Technique", *Journal of Tribology*, vol. 116, pp. 549-556.

[26] A. Almqvist, (2004), "Rough Surface Elastohydrodynamic lubrication and Contact Mechanics", PhD, Department of Applied Physics and Mechanical Engineering, Lulea University of Technology.

- [27] D. Zhu and Y. Hu, (2001), "Effects of Rough Surface Topography and Orientation on the Characteristics of EHD and Mixed Lubrication in Both Circular and Elliptical Contacts", *Tribology Transactions*, vol. 4, p. 7.
- [28] N. Patir and H. S. Cheng, (1978), "An Average Flow Model for Determining Effects of Three-Dimensional Roughness on Partial Hydrodynamic Lubrication", *ASME Journal of Lubrication Technology*, vol. 100, pp. 12-17.
- [29] C. H. Venner and W. E. Ten Napel, (1992), "Surface Roughness Effects in an EHL Line Contact", *ASME Journal of Tribology*, vol. 114, pp. 616-622.
- [30] T. Almqvist and R. Larsson, (2002), "The Navier-Stokes approach for thermal EHL line contact solutions", *Tribology International*, vol. 35, pp. 163-170.
- [31] T. Almqvist, A. Almqvist, and R. Larsson, (2004), "A comparison between computational fluid dynamic and Reynolds approaches for simulating transient EHL line contacts", *Tribology International*, vol. 37, pp. 61-69.
- [32] M. Hartinger, D. Gosman, S. Ioannides, and H. Spikes, (2005), "CFD modelling of elastohydrodynamic lubrication", Washington, D.C., pp. 531-532.
- [33] M. Hartinger, M. L. Dumont, S. Ioannides, D. Gosman, and H. Spikes, (2008), "CFD modeling of a thermal and shear-thinning elastohydrodynamic line contact", *Journal of Tribology*, vol. 130, pp. 179-180.
- [34] V. Bruyere, N. Fillot, G. E. Morales-Espejel, and P. Vergne, (2012), "Computational fluid dynamics and full elasticity model for sliding line thermal elastohydrodynamic contacts", *Tribology International*, vol. 46, pp. 3-13.
- [35] S. Srirattayawong and S. Gao, (2012), "A CFD Study of the EHL Line Contact Problem with Consideration of the Surface Roughness under Varied Loads", presented at the 9th International Conference on Heat Transfer, Fluid Mechanics and Thermodynamics, Malta.
- [36] H. Hertz, (1881), "The contact of solid elastic bodies [Über die Berührung fester elastischer Körper]", *Journal für die reine und angewandte Mathematik*, vol. 92, pp. 156-171.
- [37] K. L. Johnson, (1985), *Contact mechanics*, Cambridge: Cambridge University Press.
- [38] Y. H. Wijnant, (2005), "Contact Dynamics in the Field of Elastohydrodynamic Lubrication", Ph.D. Thesis, University of Twente, The Netherlands.
- [39] G. Gasni, M. K. Wan Ibrahim, and R. S. Dwyer-Joyce, (2011), "Measurements of lubricant film thickness in the iso-viscous elastohydrodynamic regime", *Tribology International*, vol. 44, p. 11.
- [40] L.-M. Chu, H.-C. Hsu, J.-R. Lin, and Y.-P. Chang, (2009), "Inverse approach for calculating temperature in EHL of line contacts", *Tribology International*, vol. 42, pp. 1154-1162.
- [41] S. Srirattayawong and S. Gao, (2013) "A computational fluid dynamics study of elastohydrodynamic lubrication line contact problem with consideration of surface roughness", *Computational Thermal Sciences*, vol. 5, pp. 195-213.

10. BIOGRAPHIES



Dr. Sutthinan Srirattayawong received his PhD in Mechanical Engineering (2013) from the University of Leicester, United Kingdom. Currently he is a lecturer at the University of Phayao. His research interest includes CFD analysis of the real surface roughness effects on the thermal-elastohydrodynamic lubrication and grain drying under vacuum pressure.



Dr. Rachaneewan Aungkurabut received her PhD in Mechanical Engineering (2012) from The University of Texas at Arlington, USA. Currently she is a lecturer at the University of Phayao. Her research interest includes thermal conductivity improvement for mortar using water yacinth and a full-scale biodiesel microreactor.